DIFFUSION IN HIGHLY TURBULENT FLOW THROUGH LOOSE ROCK POROUS MEDIA

by

Johannes Gessler

Prepared for

Pittsburgh Plate Glass Industries
Chemical Division
Corpus Christi, Texas

Civil Engineering Department
Engineering Research Center
Colorado State University
Fort Collins, Colorado

September 1967

CER67-68JG16

DIFFUSION IN HIGHLY TURBULENT FLOW THROUGH LOOSE ROCK POROUS MEDIA

by

Johannes Gessler

Prepared for

Pittsburgh Plate Glass Industries
Chemical Division
Corpus Christi, Texas

Civil Engineering Department
Engineering Research Center
Colorado State University
Fort Collins, Colorado

September 1967

CER67-68JG16

TABLE OF CONTENTS

LIST OF FIGURES

DIFFUSION IN HIGHLY TURBULENT FLOW THROUGH LOOSE ROCK POROUS MEDIA

by

Johannes Gessler

INTRODUCTION

In the operation of vertical lime kilns as presently used by Pittsburgh Plate Glass Industries, several operational problems arise, such as overheating the refractory lining, incomplete combustion of fuel gas, an excess amount of oxygen in the outflowing gas, and others. An improvement in the operation of the kilns seemed possible only if the basic processes in the kiln are properly understood. In particular, the diffusion process needed some clarification in connection with the occurrence of excessively high flow rates along the kiln wall (piping).

A pure theoretical treatment of the problem seemed to be impossible. Very little research had been conducted in the field of diffusion in porous media and this mainly in the range of laminar flow or to some extent in the transition range between laminar and turbulent flow. No results were available for conditions similar to those in kilns. Therefore, it was decided to run an experimental study about diffusion in porous media under highly turbulent flow conditions.

Since the diffusion process, rather than the combustion process, was to be subject of these studies, it was felt that it was not necessary to build a complete scale model of a kiln including the combustion process. The diffusion and friction laws can be investigated in a "cold" model as well as in a "hot" one. Further, it seemed desirable to use the prototype kiln feed material as the

porous medium in the study. In a complete scale model, it would also have been necessary to reduce the grain size by the scaling factor. This would have resulted in significant changes of the geometric properties of the rock material. Therefore, any geometric similarity between model and prototype kiln was foregone.

It was the aim of this study to investigate, on a basic level, experimentally and as far as possible theoretically, the diffusion and flow processes through a broken lime stone material. Therefore, it also was possible to substitute water moving through the model for the gases moving through the kiln without limiting the generality of the result. To keep the conditions in the kiln and in the model similar, only the Reynolds number must be the same. (The ratio of flow velocity multiplied by the grain size to the kinematic viscosity of the fluid). Since the kilns operate in the range of completely turbulent flow, even the Reynolds number does not influence the diffusion process significantly.

Since the basic diffusion and flow processes are studied, the direct applicability of the model results upon the kiln might be questioned. The most important difference between model study and prototype conditions is the fact that in the kiln a considerable amount of the total flow rate is injected from a source (or better, many sources) within the porous medium, while in the model study merely a tracer was injected to mark the water. From studying the lateral distribution of the tracer on a certain level it may be learned how likely it is to find a fluid particle at a specific location after released from a certain point source. How many fluid particles are released at the same time from a specific point seems, at least in a first approximation, to be unimportant. The course a particle will take is a purely probabilistic problem which depends first of all upon the

geometry of the porous medium. For these reasons, it was felt that in a first approximation it is reasonable to predict the course of the fuel in the kiln upon the course of traced water particles in the model.

The second limitation is due to the difference in geometric shape of the flow cross section. In this study, first an approach was used which enabled the determination of the diffusion process in an unconfined medium. In a second step, the influence of a wall was investigated. Due to the fact that diffusion in a porous medium is poor, for most practical purposes in kiln design it is possible to simplify the problem to the point that the injection point is close to a plane wall.

As a third limitation, it must be mentioned that only two different types of rock material were investigated. Despite significant differences in shape, the two materials produced the same result as far as diffusion is concerned. It might be assumed that shape and porosity are secondary effects in the diffusion process. This assumption is not valid, however, in the friction law where these two properties are of great importance. Since most of the operational problems are related to the diffusion process rather than to the friction law, a systematic investigation of shape and porosity influence upon pressure drop through porous media was not considered to be the main aim of this report. It will be demonstrated merely that there is such an influence. Further, these results make it possible to predict the required power to drive a given amount of air through the kiln.

In interpreting the results presented in this report these limitations should always be kept in mind. Nevertheless, it seems to us that none of these limitations is too strict to deter the applicability of the results in the design and operation of vertical lime kilns. The results are not only of a qualitative nature but also furnish reliable quantitative information.

Methods of application of these investigative results to the operational problems in a kiln will be subject of a special report furnished to PPG Industries by Dr. V. Yevjevich.

Chapter I

THE EXPERIMENTAL APPARATUS

1. The Small Model

Since not much research had been done in the field of diffusion in porous media at very high Reynolds Numbers, it was decided to build a small model first. It was the aim of the studies with the small model to develop experimental techniques to be used later in the large model.

Areas of special concern in developing techniques were:

a. Uniform flow over the inlet cross section;
b. Stable flow conditions through the rock bed;
c. Tracer injection at a very constant flow rate;
d. Method of withdrawing traced samples; and
e. Techniques for measurement of water discharge, tracer discharge, tracer concentrations, and pressure drop along the rock bed.

The design of the small model was developed from information in the literature and is shown in Figure 1.

The inlet part - A pump with a capacity of up to 0.25 cfs at heads of some 10 feet delivered a constant discharge. A bypass enabled the pump to run always at full capacity, at discharges of .25 cfs or less, without overheating. Discharge through the rock bed was measured by means of an orifice meter, calibrated at its site between the bypass and the valve, controlling discharge through the rock bed.

Before running the discharge through the packed part of the column, flow was expanded by being passed through a set of sieves

to a cross-sectional area approximately twice that of the packed pipe. The more or less homogeneous turbulence generated over the cross section by the sieves was damped out in the following tranquilization zone and the acceleration section. The remaining turbulence was insignificant compared to the disturbances induced by the grain-supporting sieve and especially by the rock bed itself. The successive passage of the water through a set of sieves, the tranquilization zone and acceleration section insured, besides the low level of turbulence, a flow uniformly distributed over the cross section.

The rock bed - The rock bed itself consisted of broken limestone of a size ranging from 0.5" to 0.75" with an assumed average of 0.625".

The shape characteristics of this material are significantly different from those of the kiln feed material. The edges are sharper, the geometric shape more arbitrary, correlation between the controlling axis and weight, or especially between the two main axes of the grain is much less pronounced.

It is suspected that these shape characteristics influence the pressure drop through the rock bed. But it seems unlikely that it would significantly influence the diffusion process, which in a first approximation should depend only upon a controlling length scale (the controlling grain size).

The rock bed in the small model was two feet deep. Along the depth there were five piezometric taps arranged to measure the pressure.

The broken rock material was carefully placed in the column so as to produce a homogeneous bed and to avoid later consolidation of the bed due to vibration during operation. If the column had not been very tightly packed, this might have resulted in piping effects

through the bed similar to those in soils under quicksand conditions, i.e., highly unstable conditions.

The outlet - The unpacked section of the column above the top screen contained the sampling device for withdrawal of traced water samples.

In a preliminary stage of the experiments, a closed conduit led back from the top of the model to the sump. This resulted in pressures lower than atmospheric pressure, at least in the upper parts of the model, causing severe problems in reaching stable flow conditions.

Therefore, the top of the model was changed to the design indicated in Figure 1. An overflow on top of the column provided stable pressure conditions in the rock bed. Then the water was run back by gravity to the sump. At the end of the return pipe it was possible to switch from recirculation through the sump to a waste line. This avoided the recirculation of traced water which would have resulted in an accumulation of tracer in the sump.

The injection apparatus - The tracer injecting apparatus is sketched in Figure 2. It consists of a tracer storage container connected to a pump (Chemcon, Model 1110) which discharged between 0.5 cm^3/s and 1.5 cm^3/s with an accuracy of ± 2%. The tracer then passed through a set of filters in order to eliminate solid particles (dye crystals) which would not pass through the narrow openings of the flow meter. Since the pump did not deliver a constant flow, but rather single strokes (at a frequency of approximately 45 strokes/minute), a flow regulator was placed in the line. The lower half of the regulator contained liquid, while the upper half contained air under pressure. Each single stroke slightly increased the pressure in the regulator. Then, between two strokes, the pressure decreased again. Since the total pressure (ambient plus

increment) varied within a narrow range which depends upon the air volume in the regulator, the outflow rate can only vary between limits dependent on the characteristics of the flow regulator. The regulator was designed to keep the flow rate variation due to the pump strokes below one percent at the injection point.

Before reaching the injection point the tracer fluid passed through a Brooks ELF turbine flowmeter. The output of the turbine flowmeter was a pulsating DC signal which was fed into a Brooks frequency - to - DC analog converter. The DC output from the converter was directly proportional to the flow rate. The flow meter was calibrated and later recalibrated in the course of these studies by sampling the tracer fluid over a given period of time.

The injection probe itself was a 1/4" stainless steel tube which entered the model through the side wall just below the rock bed. At the end of this pipe, a small 1/32" vertical pipe approximately 1/2" long was mounted, insuring that the flow direction of the injected fluid was parallel to the general direction of flow. The velocity of the injected fluid at the injection point is unimportant, since by the time the fluid reaches the first particle, the injection fluid will have assumed the same velocity as the surrounding fluid.

The sampling device - Immediately above the top screen, a rotatable arm was mounted which permitted the simultaneous withdrawal of traced fluid at six different positions along a radius. By rotating the arm to different positions it was possible to receive a set of samples representative of the tracer distribution over the total cross section.

Concentration measurements - The tracer used in this study was Rhodamine W-T red fluorescent dye. This has a high fluorescence and is not readily absorbed.

Dye concentrations were measured in a Turner Model 111 fluorometer, calibrated to prove proportionality between tracer concentration and reading at the flowmeter dial. This relation is temperature dependent. Therefore, to determine absolute concentrations it would be necessary to include temperature in calibrating the fluorometer. But since in this investigation only relative concentrations were of interest, it was possible to neglect temperature effects without inducing an error. The only requirement was to keep all samples of one experiment at the same temperature.

The initial fluorescence of the clear water was taken into account.

To increase accuracy of this measurement, the samples of traced water were diluted all into the same range of concentration. After determining the concentration of the diluted sample, this concentration was multiplied by the dilution factor to calculate the real concentration. This procedure restricted the work to a narrow range of measured concentrations where proportionality between reading and concentration was assured. Error due to dilution was well below one percent.

The reading accuracy of the fluorometer is limited to approximately ± 0.5 division of the dial. This corresponds to an error in concentration of ± 1 to 3 %. The insignificance of this error will be discussed in the chapter on evaluation of results.

2. The Large Model

The experience gained with the small model showed that no major modification of the general design was required. Only the inlet part had to be modified, since the 3' diameter of the large model and the maximum required rock bed depth of 8' would have made the model too high.

To insure a uniform flow in the vertical column after entering into the model at a right angle to the final flow direction, the flow was first passed through a heavy punched plate with circular holes. After a tranquilization section the flow passed through a similar plate supporting about 3 layers of 1" to 1.5" gravel held in place by a top screen. The energy loss through this sequence of baffles was large compared with the kinetic inlet energy and very large compared with the kinetic energy before entering the rock bed. It therefore resulted in a highly uniform flow distribution on the level of the screen supporting the rock bed.

This design made possible all those means of insuring a uniform flow within a vertical distance of only one pipe diameter.

The rock bed consisted of actual kiln feed material with the following particle size distribution:

Back rock	6%
2 - 3"	17%
3 - 4"	45%
4 - 5"	32%

This composition was furnished to Engineering Research Center by Pittsburgh Plate Glass Industries.

The material was hand placed and distributed over the cross section as uniformly as possible.

To compare this material with the material in the small model, analogous investigations were conducted in describing it. These resulted in a much higher correlation coefficient between weight and axis or between any two axes. In terms of general geometric shape, this means that there was less variation in the shape of individual grains and the grains broke more uniformly.

In other respects, especially as far as the top of the model and the injection apparatus is concerned, the large model was similar to the small one.

Chapter II

FLOW RESISTANCE THROUGH LOOSE ROCK POROUS MEDIA

1. The General Resistance Law

The velocity - pressure gradient relationship for the flow of fluids (liquid or gas) through porous media has been well investigated. One of the more recent publications on this subject is by C. R. Dudgeon, 1966[1]. This particular reference gives information even for very high Reynolds numbers ($10^3 < R < 10^4$) as they pertain to these investigations. Further, in some of the experiments by Dudgeon, very coarse material was used (river gravel up to 6", broken material up to 3"). For these reasons, Dudgeon's studies are used as reference.

The general resistance law is usually written in the form

$$\Delta p = f \frac{\rho V^2}{2} \frac{L}{k} \qquad \text{(II-1)}$$

where Δp = pressure drop,

f = friction factor,

ρ = density of fluid,

V = flow rate per unit cross-sectional area,

L = depth of porous medium bed over which the pressure drop Δp occurs, and

k = particle size of porous medium.

---

[1] Dudgeon, C. R., "An Experimental Study of the Flow of Water Through Coarse Granular Media", La Houille Blanche, No. 7, 1966.

In Eq. (II-1), the friction factor, f, is a function of the Reynolds number:

$$f = F\left(R = \frac{Vk}{\nu}\right) , \qquad \text{(II-2)}$$

where R = Reynolds number, and

ν = kinematic viscosity of fluids.

The intent of most of the experimental studies about the resistance law is to determine the function between friction factor and Reynolds number as given in Eq. (II-2).

In Figure 3, Dudgeon's results are reproduced. The general trend of the $f - R$ function can be divided into three ranges: a laminar range for which $R < 5$; a transition range for which $5 < R < 500$; and a fully turbulent range for which $R > 500$. The laminar range and part of the transition range are typical for groundwater flow. The turbulent range is rarely observed in the field and usually occurs only under artificially created conditions.

Noteworthy is the wide range of f values in the turbulent range. At $R = 1000$, f values for broken material ("blue metal") were observed ranging from as low as 20 to a maximum of 110. To some extent, this variation might be caused by different porosities. However, no systematic trend can be found in Dudgeon's observations. A more likely reason for this variation is probably difference in shape characteristics of the particles.

2. The Wall Effect Upon the Friction Law

The flow rate in a packed pipe is not uniformly distributed over the cross-sectional area. In the core of the pipe, there is a strong interlocking between the particles. Near the pipe wall, this interlocking cannot take place, since the wall is smooth. Therefore, there is an annulus at the wall with a high porosity. The difference of porosity between the core and the wall annulus depends on grain

shape and the ratio of particle size to pipe diameter. A direct observation of the core porosity and wall porosity is not possible, but for spheres in a pipe, the problem can be treated theoretically. Randomly packed spheres with a diameter of .625" in a pipe with an inside diameter of 11.5" (corresponding to the conditions in the small model) would give a wall porosity of approximately 47%, compared to a core porosity of approximately 37%.

The significantly higher porosity along the wall in an annulus about half the average grain diameter wide will result in higher velocities along the wall and therefore in a higher flow rate per unit cross-sectional area along the wall than in the core. There is little hope of any prediction of ratios of wall flow rates to core flow rates based on theoretical considerations, but there is a relationship between those two flow rates and the average flow rate over the total cross-sectional area:

$$V_w a_w + V_c a_c = V_{av} a_p \qquad \text{(II-3)}$$

where

V_w = flow rate per unit area in the wall annulus,
V_c = flow rate per unit area in the core,
V_{av} = average flow rate per unit area over total cross section of pipe,
a_w = area of the wall annulus,
a_c = area of the core, and
a_p = total cross-sectional area of pipe with radius R.

Further, the following relationships hold:

$$a_w = \pi \left(R^2 - (R - k/2)^2\right) = \pi kR \left(1 - \frac{1}{4}\frac{k}{R}\right) \qquad \text{(II-4)}$$

$$a_c = a_p - a_w = \pi R^2 \left(1 - \frac{k}{R} + \frac{1}{4}\frac{k^2}{R^2}\right) \qquad \text{(II-5)}$$

Then from Eqs. (II-3), (II-4) and (II-5), it follows

$$n = \frac{V_w}{V_c} = 1 + \frac{R}{k}\left(\frac{V_{av}}{V_c} - 1\right) . \qquad \text{(II-6)}$$

Dudgeon reports values for V_{av} / V_c of 1.10 to 1.15 for a pipe radius to particle size ratio approximately the same as in the small model. This would correspond to n-values of approximately 1.9 to 2.4 . For conditions similar to these in the large model, he got results corresponding to n-values of approximately 1.6 to 1.8 .

3. Experimental Results

In Figure 4, the friction factor is plotted against the Reynolds number for the experiments in the small and large model.

Small model - The material placed in the small model (pipe inside diameter $11\frac{1}{2}$" , depth of bed 2') was broken limestone, furnished to Engineering Research Center by Pittsburgh Plate Glass Industries, Corpus Christi, Texas. As already outlined in Chapter I, it consisted of the same material as fed to the kilns but was broken down in size to a range of $0.5" < d < 0.75"$. Due to the internal stratification of the kiln feed material, the particle shaped properties were significantly changed in the breaking process. Therefore, the results of measurements of the friction factor in the small model are not representative of the present conditions in the kilns. Nevertheless, the results from the two models demonstrate that the friction factor is shape-dependent and might change significantly in the kiln if the presently used kiln feed material is replaced by some other material.

The f-values are based upon the average velocity over the total cross section. This velocity was used as the reference velocity because it is clearly defined. The core velocity, which should

actually be used as the reference velocity, was not directly measured and its magnitude could only be estimated with an accuracy of approximately ± 10% .

The computed f - values at the highest Reynolds number reached in the small model (R = 2000) were approximately 64. Based upon the core velocity, the corresponding f - value might be as high as 85-105. The trend in Figure 4 of the observed point in the small model is in good agreement with the results in Figure 3.

Large model - The kiln feed material was delivered to the Engineering Research Center in four fractions: "Back Rock"(<2"), 2" - 3" , 3" - 4" , and 4" - 5" . In a first set of experiments, the friction factors of the 2" - 3" material and the 4" - 5" material were determined separately. Both fractions showed f - values of approximately 32-34 in a range of Reynolds numbers from 1700 - 6700. Based upon core velocity this may correspond to f - values of 42-48. It is reasonable to assume that the 3" - 4" fraction has the same average friction factor.

A second set of experiments was conducted using an artificially segregated rock bed. The cross section was split into a core part and two surrounding annuli, all with equal areas. In the core, the 4" - 5" fraction was placed; in the first annulus, the 3" - 4" fraction; and along the wall, the 2" - 3" fraction. To compute the pressure drop according to Eq. (II-1), with V as total flow rate divided by total cross section and with any of the three grain sizes as k (e.g., the intermediate grain size) first a f_{av} must be determined:

$$\Delta p = f_{av} \frac{\rho V_{av}^2}{2} \frac{L}{k_2} \qquad \text{(II-7)}$$

where

$k_1 > k_2 > k_3$, with k_1 = diameter of grains in core; k_2 = diameter of grains in first annulus; and k_3 = diameter of grains at the wall.

Equation (II-1) is valid for each segment of the pipe, where each grain size has its corresponding velocity, and the pressure drop over the rock bed as well as the depth of the rock bed are the same for all segments.

$$\Delta p = f_1 \frac{\rho V_1^2}{2} \frac{L}{k_1} = f_2 \frac{\rho V_2^2}{2} \frac{L}{k_2} = f_3 \frac{\rho V_3^2}{2} \frac{L}{k_3} \quad . \text{(II-8)}$$

From the experiments with uniform grain size, it was learned that f can be assumed to be the same for all grain sizes. Therefore, it follows that

$$\frac{V_1^2}{k_1} = \frac{V_2^2}{k_2} = \frac{V_3^2}{k_3} \quad .$$

The average velocity is given by

$$V_{av} = \frac{1}{a_p} \left(V_1 a_1 + V_2 a_2 + V_3 a_3 + V_3 (n-1) a_w \right) \qquad \text{(II-9)}$$

where

a_1, a_2, a_3 are the cross-sectional areas of the segments with grains of diameter k_1, k_2, and k_3 respectively;

a_w is the area along the wall over which piping takes place;

n is the ratio of the velocity at the wall in the piping area to the velocity outside the piping area.

Now it follows that:

$$f_{av} = 2 \Delta p \frac{1}{\rho V_{av}^2} \frac{k_2}{L} = 2 \Delta p \frac{1}{\rho V_1^2} \frac{k_1}{L} \left(\frac{V_1}{V_{av}} \right)^2 \cdot \frac{k_2}{k_1}$$

$$\frac{f_{av}}{f_1} = \left(\frac{V_1}{V_{av}}\right)^2 \cdot \frac{k_2}{k_1} \qquad \text{(II-10)}$$

The ratio $\left(V_{av}/V_1\right)$ follows from Eq. (II-9) with

$$a_w = \pi R k_3$$

$$\left(\frac{V_{av}}{V_1}\right)^2 = \frac{1}{9}\left[1 + \sqrt{\frac{k_2}{k_1}} + \sqrt{\frac{k_3}{k_1}}\left(1 + (n-1)\frac{3k_3}{R}\right)\right]. \qquad \text{(II-11)}$$

It is seen from Eqs. (II-10) and (II-11) that for no piping ($n = 1$), $f_{av}/f_i \simeq 1.0$, using k_2 as the reference grain size. Also, for small values of k_3/R, $f_{av} \simeq f_i$. For practical purposes, in the kiln f_{av} might be assumed to be equal to f_i, if the material is artificially segregated and a medium grain size (i.e., $\frac{1}{2}\left(k_{min} + k_{max}\right)$ is used as the reference size.

In the experiments with artificially segregated material, values of f_{av} were observed of approximately 22 (at $R = 3500$) ; f_i was estimated to be approximately 42. Whether this ratio f_{av}/f_i is reasonable is difficult to determine due to the difficulties in estimating n. According to Eqs. (II-10) and (II-11), the observed values would require n-values of approximately 4, which seems to be unreasonably high. Nevertheless, a method to evaluate n, to be developed later, indicates n-values of almost this magnitude in the small model in some tests. Due to the difficulties in packing the tube with segregated material, it might have happened that there was some additional piping in the boundaries between one grain size and the next. This would have led to a further reduction of f_{av} and might explain the observed low f_{av}-values.

Finally, in all experiments with the kiln feed material, the friction factor was computed from the observed pressure drop.

A representative sample of kiln feed material was assembled at the Engineering Research Center from materials supplied by Pittsburgh Plate Glass Industries, in the proportions specified by the Company (see Chapter I). Since each individual grain contributes to the total pressure drop over the depth of the rock bed, it is reasonable to compute an average grain size from the number of grains of each size in the sample:

$$k_{av} = \frac{1}{\Sigma_i m} \left(k_1 m_1 + k_2 m_2 + \ldots k_i m_i \right) \qquad \text{(II-12)}$$

where m_i = number of grains in fraction i .

The number of grains in one fraction can be estimated under the assumption that the grains can be approximated by spheres:

$$m_i = \frac{\text{total weight of fraction i}}{\pi \, k_1^3 / 6} \; .$$

This results in a $k_{av} = 2.5''$ for the kiln feed material sample used in the tests.

The measured friction factors are mostly in the range between 30 and 35 at a Reynolds number of approximately 3500. This indicates that the average friction factor of the mixture is identical with the friction factor of the individual fractions if k_{av} is computed according to Eq. (II-12).

Based upon core velocity, the friction factor might be somewhere between 40 and 50.

Chapter III

DIFFUSION FROM A FIXED SOURCE

1. Theoretical Considerations

Diffusion in an unconfined medium - If it is considered that the loose rocks of the porous medium are oriented randomly and that the rock bed has a constant porosity throughout the flow field, i.e., if the porous medium is homogeneous and isotropic, it should be possible to treat the diffusion process as diffusion in a homogeneous isotropic turbulence field. Except in the immediate vicinity of the source, it is reasonable to assume long diffusion times. The differential equation for the mean concentration then reads

$$V \cdot \frac{dC}{dx_1} = \epsilon \frac{d^2}{dx_i\, dx_i} C \quad . \tag{III-1}$$

The solution for a continuous point source is

$$C = \frac{S}{4\pi r_s \epsilon} \exp\left[- \frac{V (r_s - x_1)}{2\epsilon} \right] \tag{III-2}$$

where C = concentration of tracer,

S = strength of tracer source,

$r_s = \sqrt{x_1^2 + x_2^2 + x_3^2}$,

ϵ = diffusion coefficient,

V = mean flow velocity in x_1-direction (flow rate per unit area),

x_i = orthogonal coordinates of the point with concentration C (origin at injection point and x_1-direction as flow direction).

This solution can be simplified if $x_2^2 + x_3^2 \ll x_1^2$, i.e., if $r_s/x_1 \simeq 1$. This condition holds in the planned experiments. Eq. (III-2) simplifies to

$$C(x_1 , r) = \frac{S}{4\pi x_1 \epsilon} \exp \left[- V \frac{r^2}{4\epsilon x_1} \right] \qquad \text{(III-3)}$$

where

$$r = \sqrt{x_2^2 + x_3^2} \quad .$$

The diffusion coefficient is determined by

$$\epsilon = v_2' \quad \Lambda_L \qquad \text{(III-4)}$$

where

v_2' = root mean square of the lateral velocity fluctuation,

and

Λ_L = Lagrangian integral length scale.

Due to the unique situation in a porous medium, it is possible to make reasonable assumptions concerning the lateral fluctuations and the characteristic length scale.

The lateral velocity fluctuations - The root mean square of the lateral velocity fluctuation in a turbulent field corresponds here to the average absolute value of the lateral velocity component. Such a component exists because the geometric arrangement of the grains force the flow through the voids which are randomly oriented. For this reason, the average lateral velocity component must be directly proportional to the average mean flow velocity:

$$v_2' = c_1 V \quad . \qquad \text{(III-5)}$$

To evaluate the constant c_1 , it must be kept in mind that the real velocity in a void is a maximum if the void is vertically oriented. In horizontal voids, the velocity will usually be very small since there is no significant pressure drop from one end of the void to the other.

Therefore, those voids with high velocities will contribute only little to the lateral component, since the flow direction is almost vertical, while the more horizontal voids contribute little to the lateral velocity component since the velocity in the void is small. For these reasons, it is to be expected that c_1 must be significantly smaller than unity. A more detailed investigation leads to a value of c_1 of approximately 0.5 .

Lagrangian integral length scale - The Lagrangian integral length scale indicates as an average how far a fluid particle may travel keeping approximately the same direction. It is obvious that this distance will be directly proportional to the grain size:

$$\Lambda_L = c_2 k \quad . \tag{III-6}$$

For spheres, packed as densely as possible (porosity $n = 0.26$), this traveling distance is $k/3$ (k sphere diameter). But since the porosity in the kiln is as high as approximately 0.41, it is necessary to adjust Λ_L accordingly. If the porosity becomes greater, it is obvious that the distance between the void centers increases proportionally to $1/\sqrt[3]{1-n}$. Hence, it is reasonable to replace Eq.(III-6) by

$$\Lambda_L = \frac{c_2' k}{\sqrt[3]{1-n}} \tag{III-7}$$

The fact that for $n = 0.26$ Λ_L becomes $k/3$ leads to $c_2' \simeq 0.3$. Together with $n = 0.41$ for kiln feed material, the length scale becomes approximately

$$\Lambda_L \simeq 0.36\, k$$

Combining Eqs. (III-5) and (III-6) yields

$$\epsilon = c_1 c_2 V k \tag{III-8}$$

It is expected with $c_1 \simeq 0.5$ and $c_2 \simeq 0.36$ that the product $c_1 c_2$ will be in the range of 0.15 to 0.20 .

Replacing the diffusion coefficient ϵ in Eq. (III-3) with the value given in Eq. (III-8) leads, after some rearrangement, to

$$\pi \frac{C}{S} V k x_1 = c_3 \exp \left[- c_3 \frac{r^2}{k x_1} \right] \qquad \text{(III-9)}$$

where

$$c_3 = \frac{1}{4 c_1 c_2} \quad .$$

The value of c_3 is dimensionless and expected to be in the range between 1.2 and 1.7 . The exact value must be determined experimentally. It is not a constant for all types of material since it is shown in Eq. (III-7) that it depends, at least, upon the porosity.

In Eq. (III-9), the terms are arranged in two dimensionless groups, a dimensionless parameter which is proportional to the concentration

$$\pi \frac{V k x_1}{S} C$$

and a dimensionless parameter which is proportional to the distance between the injection axis and the point with concentration C

$$\frac{1}{\sqrt{k x_1}} r \quad .$$

The presentation of the diffusion equation by means of two dimensionless parameters has the tremendous advantage that it represents the concentration distribution on any level x_1 , in any type of material, for any velocity V and strength of source S (except for possible slight variations in c_3) .

Linearity Principle

The first of these two dimensionless parameters proves the linearity principle. If the concentration is observed at a given point

in a given material (i.e., for given x_1 and k), the right side of Eq. (III-9) remains constant, and therefore,

$$\frac{CV}{S} = \text{const.}$$

In other words, for a given strength, S , a doubling of the velocity will lead to reduction of the concentration by a factor of 2 ; or, for a given velocity V , the concentration is proportional to the strength of the source.

Velocity Independence

Equation (III-9) represents a Gaussian distribution of the concentration profile. Although there is no finite distance from the injection axis over which C becomes zero, a measure for the width of the concentration profile is the standard variation σ . Comparison of the power of e in Eq. (III-9) with the power of e in the standard form of a Gaussian distribution will lead to

$$\frac{r^2}{2\sigma^2} = \frac{c_3 r^2}{kx_1}$$

or

$$\sigma = \sqrt{\frac{1}{2c_3}} \sqrt{kx_1} \quad . \qquad \text{(III-10)}$$

The tangent of the angle of the diffusion cone (the cone above the injection point in which the highest concentration of tracer will be found) might be defined by

$$\tan \rho = \frac{\sigma}{x_1} = \sqrt{\frac{1}{2c_3}} \sqrt{\frac{k}{x_1}} \quad . \qquad \text{(III-11)}$$

Equation (III-11) clearly shows that this cone is independent of velocity. In other words, the shape of the concentration profile on a given level does not depend upon the velocity. The absolute concentration, C , however, depends upon the velocity according to the linearity principle.

Linear Superposition

The principle of linear superposition is generally accepted in diffusion processes. It states nothing but the independence of the diffusion process from one source upon possible sources in the neighborhood. Each source can be treated individually. The absolute concentration at a point due to several injection points then is obtained by adding the corresponding absolute concentrations from the individual sources.

Diffusion in the Vicinity of a Plane Wall

If there is a wall in the vicinity of the injection point, the part of tracer which would be beyond the wall in the unconfined medium will be reflected back into the half space in which the source is positioned. The effect is that of an imaginary source, the mirror image of the primary source, having the same strength, with no wall between the two. That is, the wall behaves as a mirror. And the concentrations due to one source in the vicinity of the wall can be computed by superimposing the unconfined concentration distribution from the real and the imaginary source (Fig. 5).

The position of the source with respect to the wall is given by the distance from the wall, a. The position of P is given by r and x_2. From these three variables, r'^2, the square of the distance between P and the imaginary source can be computed:

$$r'^2 = r^2 + 4a\,(a - x_2) \quad . \tag{III-12}$$

The concentration at P due to the primary source in the unconfined medium is given by

$$C_p \frac{Vkx_1}{S} \pi = c_3 \exp\left[- c_3 \frac{r^2}{kx} \right] \quad . \tag{III-13}$$

The concentration at P due to the imaginary source in the unconfined medium (the concentration due to wall reflection) is given by

$$C_s \frac{Vkx_1}{S} \pi = c_3 \exp\left[- c_3 \frac{r^2 + 4a\,(a-x_2)}{kx_1} \right] . \quad \text{(III-14)}$$

The concentration at P in the confined medium is now

$$C_c = C_p + C_s$$

or

$$C_c \frac{Vkx_1}{S} \pi = c_3 \exp\left[- c_3 \frac{r^2}{kx_1} \right] \left\{ 1 + \exp\left[- c_3 \frac{4a\,(a-x_2)}{kx_1} \right] \right\} \quad \text{(III-15)}$$

To evaluate the wall effect, it is reasonable to compute the ratio of the concentration at P in the confined medium, C_c, to the concentration at P in the unconfined medium, C_p:

$$\frac{C_c}{C_p} = 1 + \exp\left[- c_3 \frac{4a\,(a-x_2)}{kx_1} \right] . \quad \text{(III-16)}$$

E.g., a 15% difference between the concentration at a point in the confined medium and the same point in the unconfined medium will lead to

$$a - x_2 = \frac{1.9}{4c_3} \frac{kx_1}{a} . \quad \text{(III-17)}$$

An even better measure of the wall effect is to compute how far the lines of equal concentration are shifted due to the presence of the wall compared to the condition in the unconfined medium.

In Figure 6, the lines of equal concentration are plotted on a level 8 feet above the injection point, which is 1.5 feet from the wall. The assumed grain size is 3.2 inches, the controlling grain size of the kiln feed material used in this study. The maximum concentration on this level in the unconfined medium is used as reference. In the

area left of the dashed line, the shift is less than half a grain size and therefore can be considered as insignificant. There is only a very narrow area not more than 1.5 grain diameter wide, along the wall, in which the wall affects the concentration distinctly.

Finally, it should be noted that at the wall, i.e., $x_2 = a$, according to Eq. (III-16)

$$\frac{C_c}{C_p} = 2 \quad .$$

This means that the concentrations at the wall are just twice those along the same line in the unconfined medium.

The Effect of Piping Along the Plane Wall Upon the Diffusion Process

As mentioned in Chapter II, the flow rate per unit area along the wall is significantly higher than in the rest of the porous medium. The width of this area along the wall is approximately half an average grain size. This fact will lead to a higher dilution at the wall or a reduction of tracer concentration. But to produce any reflection of tracer by the wall, the concentration at the wall must be higher than the concentration at that point in the unconfined medium.

The amount of tracer passing through that part of an unconfined medium which is on the same side of the wall as the source, excluding the piping area, is given by

$$S_{in} = V C_o \sigma^2 2\pi \frac{1}{\sqrt{2\pi}} \int_{-\infty}^{+\frac{a-k/2}{\sigma}} \exp\left[-\frac{x^2}{2}\right] dx.$$

Using the total strength of the source

$$S = V C_o \sigma^2 2\pi$$

as reference, it follows that

$$\frac{S_{in}}{S} = \frac{1}{\sqrt{2\pi}} \int_{-\infty}^{\frac{a-k/2}{\sigma}} \exp\left[-\frac{x^2}{2}\right] dx \quad . \quad \text{(III-18)}$$

The amount of tracer carried through the piping area may now be calculated under the assumption that the concentrations at the wall are equal to those along the same line in the unconfined medium, that is, the situation when reflection starts to take place. The concentration profile along the wall then is

$$C = C_o \exp\left[-\frac{(a-k/2)^2 + x_3^2}{2\sigma^2}\right] .$$

The amount of tracer carried through the piping area along the wall is

$$S_w = n\,V\,C_o \exp\left[-\frac{(a-k/2)^2}{2\sigma^2}\right] \int_{-\infty}^{+\infty} \exp\left[-\frac{x_3^2}{2\sigma^2}\right] dx_3$$

or

$$\frac{S_w}{S} = \frac{n}{2\sqrt{2\pi}} \frac{k}{\sigma} \exp\left[-\frac{(a-k/2)^2}{2\sigma^2}\right] . \quad \text{(III-19)}$$

The difference $1 - \frac{S_{in} + S_w}{S}$ indicates how much of the total tracer flow is reflected at the wall. Assuming a source 1.5 feet from a plane wall and rock bed material as presently used in the kiln, no reflection takes place up to a height of 4.5 feet. On a 6 foot level, less than 1% and on a 8 foot level, only 2.3% of the total tracer flow is reflected (n is assumed to be approximately 2). If no piping occurs, the amount of tracer reflected at the 4.5 foot, 6 foot and 8 foot levels would be 1.8%, 3.5%, and 5.9%, respectively.

The Piping Effect Upon the Diffusion Process in a Circular Pipe

To evaluate under which conditions a porous medium in a column can be considered as an unconfined medium (with the injection point in the center of the pipe), similar considerations as in the preceding paragraph will be carried out here in the case of a circular column.

The amount of tracer passing through the cross-sectional area of the column in the unconfined medium, excluding the piping area at the wall, is

$$S_{in} = V C_o 2\pi \int_o^{R-k/2} r \exp\left[-\frac{r^2}{2\sigma^2}\right] dr$$

where R is the pipe radius. Or again, with the total strength of the source as reference,

$$\frac{S_{in}}{S} = 1 - \exp\left[-\frac{(R - k/2)^2}{2\sigma^2}\right] . \qquad \text{(III-20)}$$

The amount of tracer carried through the piping area accordingly is

$$S_w = n V C_o \pi R k \left(1 - \frac{k}{4R}\right) \exp\left[-\frac{(R - k/2)^2}{2\sigma^2}\right]$$

or

$$\frac{S_w}{S} = n \frac{Rk}{2\sigma^2} \left(1 - \frac{k}{4R}\right) \exp\left[-\frac{(R - k/2)^2}{2\sigma^2}\right] . \qquad \text{(III-21)}$$

Using Eqs. (III-20) and (III-21), it is possible to evaluate how much dye will be reflected by the wall. Assuming a column diameter of 3 feet and a rock bed material as presently used in the kiln, no reflection will occur up to a level of about 3.3 feet. At the 6 foot and 8 foot levels, approximately 8% and 17%, respectively, are reflected. From the reflected part, however, a considerable amount will be

carried through the piping area due to the high velocities. Therefore, even with relatively high percentages, the tracer will not be reflected very far into the porous medium. A more detailed analysis showed that, under specific conditions as mentioned above, the reflected tracer will reach back into the porous medium not more than about 1.5 grain diameters at the 6 foot level.

In a column such as the large model (3 foot diameter) packed with a material as presently used in the kiln, the diffusion process is the same as in an unconfined medium up to a depth of 6 feet, if a wall annulus of approximately 1.5 controlling grain diameter ($\sim 5''$) is excluded from consideration. At the 8 foot level, there might be some wall influence noticeable at a distance from the wall of 5" . But this influence will probably be small compared with other errors.

It should be understood that the evaluations of the piping effect at the wall upon diffusion are not exact solutions but merely first approximations. As long as the piping effect itself is not completely understood and thoroughly investigated, there is not much justification for searching for a exact solution of this piping effect upon the diffusion close to the wall. In the presented figures it has been assumed that the flow rate per unit area is approximately twice the corresponding value in the core. The width of the annulus over which piping occurs was assumed to be half a controlling grain size.

The suitability of the assumptions will be verified, to some extent, by the experiments.

Controlling Grain Size

If the porous medium does not consist of a uniformly sized material but rather represents a mixture of different grain sizes, the problem of defining an average or controlling grain size arises.

The grain size enters into the diffusion equation through the diffusion coefficient which is proportional to the Lagrangian integral length scale. It was assumed that this length scale is proportional to the grain size. As mentioned earlier, the length scale indicates how far a fluid particle travels in an approximately uniform direction. If there are grains of different sizes, the length scale indicates the average step length. Since the number of steps of equal length is proportional to the number of grains of corresponding size, it is logical to assume the average controlling length scale to be proportional to the average grain size based upon the number of grains of each size. This is the same definition of average grain size as used in the friction law (see Eq. (II-12)).

2. Experimental Verification of the Diffusion Equation in Unconfined Media

Six experiments in the small model were carried out. In the beginning, these experiments were considered as preliminary runs to develop experimental techniques. Since the design of the small model was a complete success and no modifications of any importance with respect to the diffusion process were required, there was no reason to omit the results of these experiments in the final evaluation. They all were conducted with the injection point in the center of the column and with a bed depth of 2'. The controlling grain size was assumed to be 0.625".

In the large model, five experiments were arranged with the injection point in the center at depth of 2', 4', 6' (two experiments), and 8', respectively. The controlling grain size was computed according to Eq. (II-12), using the grain size distribution as given in Chapter I. But here the back rock fraction was omitted in the computation. This fraction is relatively small (6% of the total, by

weight) and its grains are significantly smaller than the next larger size (2-3"). Therefore, the back rock merely filled the voids between the larger particles, without contributing much to the total volume of the mixture. Therefore, the back rock fraction did not influence the diffusion process significantly.

Measured Quantities

Besides the geometric definition of the observation points (r = distance from the injection axis, x_1 = distance between the observation plane and the injection point) and the geometric description of the material (k = controlling grain size), the concentration at the observation point, the strength of the tracer source and the core velocity must be known in order to compute the two dimensionless parameters

$$\pi \frac{C}{S} V_c k x_1 \quad \text{and} \quad \frac{r}{\sqrt{k x_1}}$$

in Eq. (III-9).

The measuring techniques for determination of the concentration were covered in Chapter I and do not need further explanation. The measurement was accurate within 1% to 3%. But, as explained earlier, a direct observation of the core velocity was not possible. Therefore, the first of the two dimensionless parameters had to be modified.

The strength of the source, S , can be computed from the observed water discharge, Q , and the observed average concentration $C_{av\ ob}$

$$S = C_{av\ ob}\ Q \ . \qquad \text{(III-22)}$$

The average observed concentration was obtained by withdrawing a sample form the waste line where water and tracer were assumed to have been completely mixed. By definition of the average flow rate per unit area, it holds that

$$Q = V_{av} \pi R^2 \quad . \tag{III-23}$$

Introducing Eqs. (III-22) and (III-23) into the dimensionless parameter to be modified yields

$$\pi \frac{C}{S} V_c k x_1 = \frac{C}{C_{av\,ob}} \frac{V_c}{V_{av}} \frac{k x_1}{R^2} \quad . \tag{III-24}$$

If the diffusion process is assumed to take place in a unconfined medium where the flow rate per unit area corresponds to the core velocity throughout the medium, the strength also can be computed as

$$S = V_c \int^a C dF \quad . \tag{III-25}$$

The integral must be taken over the total cross-sectional area, a . By defining a fictitious, theoretical average concentration,

$$C_{av\,th} = \frac{\int^a C dF}{\pi R^2} \quad ,$$

Eq. (III-25) reads

$$S = V_c C_{av\,th} \pi R^2 \quad .$$

Combined with Eqs. (III-22) and (III-23), it follows

$$C_{av\,ob} V_{av} = C_{av\,th} V_c \quad . \tag{III-26}$$

and hence, it holds for the dimensionless parameter

$$\pi \frac{C}{S} V_c k x_1 = \frac{C}{C_{av\,th}} \frac{k x_1}{R^2} \quad . \tag{III-27}$$

The theoretical average concentration must be determined from integrating the observed concentration distribution. In this way, a direct measurement of the core velocity is avoided. Further, the direct determination of the strength of the source with its inherent possibility of error is unnecessary. Since the injected tracer was a dye solution, rather than pure dye, the determination of the source strength involved a flow rate measurement of the injected liquid as well as a dye concentration measurement. So far as error propagation is concerned, this procedure would have been relatively unfavorable.

Evaluation Procedure

A preliminary plotting of the measured concentrations against the distance from the injection axis showed that the concentration profile could be fitted very well by a Gaussian distribution, but that there was considerable scatter of the individual observed points. This scatter is directly related to the structure of the porous medium. The flow through the porous medium is not continuously distributed but takes place only through the voids. It must be assumed that due to the turbulence in the voids, concentration over the cross section of one void is constant, but changes from one void to the next. Therefore, no continuous dye concentration profile exists. While no concentration is defined at points which are covered by a grain, the concentration is distributed stepwise over the voids. Depending upon the structure of the voids, there might be considerable variation in concentration from one void to the next. Only the average over many voids which have the same distance from the injection axis can be expected to follow the predicted diffusion equation.

In these experiments, samples were always taken from four points equidistant from the injection axis. (From two diameters,

perpendicular to each other). In the evaluation, only the average of these four samples was used. In the small model, samples were withdrawn from 6 positions with different distances from the injection axis. In the large model, this was done from 7 positions. In both models, one of the sampling points was at the wall and was therefore omitted from the evaluation.

In order to determine the dimensionless parameter proportional to the concentration, $C_{av\ th}$ had to be computed. A direct integration of the observed distribution would have been possible only in a few experiments where no dye at all reached the wall. In experiments where some dye was carried through the piping area, this direct integration would have produced erroneous results. Therefore, it was reasonable to compute the best fit line through the observed points and to integrate this best fit distribution in order to get $C_{av\ th}$.

The computation of the best fit line made use of the fact that one half of a Gaussian distribution plots as a straight line on a graph where the ordinate value is the logarithm of the observed quantity, and the abscissa value is the square of the measured distance. Therefore, on a plot of log C versus r^2 the straight best fit line was computed according to the least squares method. This line goes through the center of gravity of the log C - r^2 - points and has a slope m. With the new variables $y = \log C$ and $x = r^2$ the center of gravity of the observed points is at

$$\bar{y} = \frac{\Sigma y}{n} \quad \text{and} \quad \bar{x} = \frac{\Sigma x}{n}$$

where n is the number of observation points. The slope m is

$$m = \frac{\Sigma (x - \bar{x})(y - \bar{y})}{\Sigma (x - \bar{x})^2} .$$

This slope is directly related to the standard deviation of the distribution function:

$$\sigma = \sqrt{\frac{0.217}{|m|}} \quad .$$

The absolute value of m must be taken, since m has a negative value. It follows that the logarithm of the maximum concentration at the injection axis according to the best fit line is

$$\log C_o = \bar{y} - m\bar{x} \quad .$$

The theoretical average concentration is computed by an integration of the best fit distribution:

$$C_{av\ th} = \frac{S}{\pi R^2} = 2C_o \frac{\sigma^2}{R^2} \quad .$$

In this manner, it was possible to compute the two dimensionless parameters for each observation point (representing an average of four measurements) and to plot all these points in one single graph (Figure 7). Included are the measurements of both the small and large models.

Since the two different materials in the small and large model, respectively, do not necessarily give the same result, the best fit curves were computed separately through the points of each model:

$$\text{Small model:} \quad \pi \frac{C}{S} V_c k x_1 = 1.42 \exp\left[-1.43 \frac{r^2}{k x_1}\right] \quad \text{(III-28a)}$$

$$\text{Large model:} \quad \pi \frac{C}{S} V_c k x_1 = 1.40 \exp\left[-1.34 \frac{r^2}{k x_1}\right] \quad \text{(III-28b)}$$

As shown in the development of the diffusion equation, the coefficients in front of the exponential function and in the power of the exponential function, respectively, are necessarily the same. This condition is excellently fulfilled in the results of the small model, while in the

large model there is a 4% deviation between the two values. Now the question might be brought up as to which is the function in the large model with the two coefficients the same, but which deviates as little as possible from the computed best fit line. The best fit function which fulfills this additional condition is:

$$\pi \frac{C}{S} V_c k x_1 = 1.42 \exp \left[-1.42 \frac{r^2}{k x_1} \right] . \qquad \text{(III-28)}$$

This function deviates from the best fit line obtained from the large model by not more than ± 0.02, a value which is negligible compared with the scatter of observed points. Therefore, it might be stated that the two models gave very nearly the same result. Equation (III-28) is plotted in Figure 7.

Comparing Eq. (III-28) with Eq. (III-9), it is found that the value c_3 determined experimentally is 1.42 and well within the predicted range of 1.2 to 1.7 .

It should be noted that the fact of possible approximation of the measured points by Eq. (III-28) is the experimental verification of the previously stated velocity independence of the diffusion process as well as the linearity principle.

3. Experiments About Diffusion in the Vicinity of a Wall

It has been demonstrated in this chapter that the diffusion from a source which is only 1.5 foot from the wall is not yet significantly influenced by the wall on a level 8 feet above the injection level except for a region along the wall which is approximately 1.5 grain diameter wide.

In the kiln, this situation is even more pronounced. Due to the high velocities in the piping area, there is always an excess of oxygen available which enables the spontaneous combustion of any

fuel reaching the area over which piping takes place. It certainly might be assumed that no unburned fuel is reflected.

For these reasons, experiments specifically investigating the reflecting effect of the wall are not of practical importance, except for the case in which the injection point is at the wall.

Injecting an inactive gas (e.g., cold exhaust gas) along the wall might be a means of reducing the wall temperatures. This exhaust gas would replace some of the fuel-oxygen mixture in the piping area, resulting in a reduction of fuel combustion in the immediate vicinity of the wall. At the same time the heating of the injected cold exhaust gas would develop a cooling effect.

It must be kept in mind that some of the injected cold gas will be lost due to diffusion into the porous medium before it reaches the wall area to be protected. To study this type of diffusion process, experiments were conducted with the injection point at the wall. The result is plotted in Figure 8, using the same dimensionless parameters as in the diagram for unconfined media.

The solid line represents the theoretical distribution for an injection point at a plane wall (according to Eq. (III-15)). That is, the ordinate values are twice these in the unconfined media. The plotted points are not corrected for the piping effect, since a correction procedure would be based upon too many assumptions. Generally speaking, however, such a correction would result in an upward shift of the points by a factor ranging from 1.5 (on the 2 foot level) to 1.25 (on the 8 feet level). This would result in an even better fit between theory and observation for values of $r/\sqrt{kx} > 0.7$. The considerably larger scatter in this figure compared with the results in the unconfined media (Figure 7) is caused by the fact that here each point represents an average of only two measurements, while in the unconfined media it was an average of four points.

The extreme deviation of the measurements in the immediate vicinity of the injection axis is certainly caused to some extent by the fact that the theory is developed for a plane wall (an assumption which is very reasonable in a kiln with a radius of 7.5 feet), while in the model the radius was only 1.5 feet. This must result in higher concentrations above the injection point. This increase should not be more than perhaps 20 - 30% , compared with an increase of approximately 100% in the model if the piping effect is taken into account.

It must be concluded that the piping effect along the wall influences the diffusion process tremendously in the immediate vicinity of the injection axis and that the theoretical considerations overestimate the diffusing tendency of a fluid injected into the piping area.

Generally speaking, it can be stated that the experimental results support the theory based upon the mirror principle, except for the immediate vicinity of the injection axis where the piping effect disturbs the process.

4. Experimental Verification of the Law of Superposition

In the large model, the law of superposition was verified. The bed configuration used to prove it was the four foot deep bed with artificially segregated material as described in Chapter II. Any other bed configuration could have been used, except perhaps for the fact that for segregated material the validity of the law of superposition is somewhat less obvious.

Two experiments were run with a single injection point at different locations. According to linear superposition for simultaneous injection at both points, it should hold that:

$$\frac{C}{C_{av}} = \frac{1}{2}\left(\frac{C_1}{C_{av_1}} + \frac{C_2}{C_{av_2}}\right) \qquad \text{(III-29)}$$

if the two sources for simultaneous injection are of the same strength.

This distribution according to Eq. (III-29) is compared in Figure 9 with the actual observation for simultaneous injection. The deviation between the two curves is small compared with grain sizes, the law can be considered as proved.

5. Some Remarks on the Scatter of Observed Measuring Points

Equation (III-9) can be written in the form

$$C^* = c_3 \exp\left[-c_3 r^{*2}\right] \qquad \text{(III-30)}$$

where C^* and r^* represent the dimensionless parameters as used as ordinate and abscissa values, respectively, in Figure 7.

In order to evaluate the expected scatter of observed points, it must be kept in mind that the theoretical concentration profile, representing the expected average concentration at a certain distance from the injection axis, can be easily shifted in either direction by about half a grain size. This is due to the discontinuous structure of the porous medium. Therefore, the expected scatter in C^* is

$$\Delta C^* = \pm \frac{dC^*}{dr^*} \frac{k^*}{2} \qquad \text{(III-31)}$$

where $k^* = \frac{k}{\sqrt{kx_1}} = \sqrt{\frac{k}{x_1}}$ is the dimensionless grain size.

Introducing the derivative of Eq. (III-30) into Eq. (III-31) results in

$$\Delta C^* = \pm c_3 r^* \sqrt{\frac{k}{x_1}} \exp\left[-c_3 r^{*2}\right] .$$

At a given distance r^* , the scatter is proportional to $\sqrt{k/x_1}$. This value was approximately 0.16 in the small model, but reached from 0.18 to 0.37 in the large model. Therefore, the scatter of the measured points in the large model is significantly larger, and the coefficients as determined in Eq. (III-28b) are less accurate than those in Eq. (III-28a) from the small model.

Chapter IV

AN EVALUATION OF THE DIFFERENCE BETWEEN CORE VELOCITIES AND WALL VELOCITIES

From the preceding chapters, it is obvious that it is of some importance to know how strong the piping effect is along the wall. Equation (III-26) gives a means of estimating the ratio of average velocity over core velocity:

$$\frac{V_{av}}{V_c} = \frac{C_{av\ th}}{C_{av\ ob}} \quad .$$

Together with Eq.(II-6), it follows that

$$n = \frac{V_w}{V_c} = 1 + \frac{R}{k}\left(\frac{C_{av\ th}}{C_{av\ ob}} - 1\right) \quad . \qquad \text{(IV-1)}$$

Equation (IV-1) makes it obvious that the accuracy of determining n by this means is very limited. The ratio of $C_{av\ th}$ to $C_{av\ ob}$ is only 10% to 30% larger than unity. A 5% error in this ratio, therefore, would result in a 20% to 50% error in the second term of the sum in Eq. (IV-1). The resulting error in n will range from ± 10% to ± 40%.

Nevertheless, the n values were computed in all experiments. While the small model gave unreasonably high values of approximately 4, the large model showed values of approximately 1.8. We can only speculate upon the cause for the small model result. It might be in connection with the significantly different shape characteristics of the material, resulting in a wider annulus over which piping takes place. It would not be surprising if, due to

the more elongated shape of these grains, the width of the annulus would be a full average grain size. Under this assumption, the n value would only be approximately 2.

The results of the large model seem reasonable and are of specific importance since they were gained from experiments using actual kiln feed material. An attempt was made to measure the wall velocity directly using a Delf-Propeller-Meter. The result is not conclusive since the propeller meter operated over the core of the column at velocities close to the minimum velocity measurable with this device. The indication at the wall was approximately 8 cm/s, while in the core a value of approximately 3.5 cm/s was observed. This would result in an n value of approximately 2.3 .

Taking the results from this study and those from Dudgeon (see Chapter II), it seems reasonable to assume a value $n = 2$ over a width of half an average grain size until better information is available.

Chapter V

DIFFUSION FROM A WALL SOURCE CONSIDERING THE WALL PIPING EFFECT

Upon the results from the diffusion experiments and their evaluation in the light of piping, an attempt will be made to develop a procedure for predicting the diffusion from a source at the wall and the influence of the piping effect upon it. The procedure to be developed will be only a first approximation of a very complex process. The point of special interest is the behavior of the injected fluid along the wall and not actually the diffusion of some parts of the injected fluid into the porous medium.

The result of this chapter will make it possible to estimate how much cold exhaust gas should be recirculated to reduce wall temperatures by a certain amount.

If a certain amount of fluid (S_c) is injected at the wall and no piping occurs, the concentration distribution is

$$C = \frac{S_c}{\pi V_c k x_1} \; 2.84 \; \exp\left[-1.42 \frac{r^2}{k x_1}\right] \qquad \text{(V-1)}$$

where $r^2 = x_2^2 + x_3^2$ with x_2 and x_3 the orthogonal coordinates perpendicular to the direction of flow and x_3 in the direction of the wall. The concentration distribution along the wall ($x_2 = 0$) then is given by

$$C = \frac{S_c}{\pi V_c k x_1} \; 2.84 \; \exp\left[-1.42 \frac{x_3^2}{k x_1}\right] \qquad \text{(V-2)}$$

It is assumed that this concentration profile given by Eq. (V-2) also holds for the strip along the wall over which piping takes place.

Then the amount of injected fluid traveling along the wall is given by the integral over C multiplied by the local velocity, i.e., the wall velocity:

$$S_w = V_w \int_{-\infty}^{+\infty} C \cdot \frac{k}{2} \, dx_3 \qquad \text{(V-3)}$$

Introducing Eq. (V-2) into Eq. (V-3) will yield

$$S_w = n \frac{S_c}{2\pi x_1} \int_{-\infty}^{+\infty} 2.84 \exp\left[-1.42 \frac{x_3^2}{k\, x_1}\right] dx_3$$

where $n = V_w/V_c$. After carrying out the integration and after some rearrangement, one obtains

$$\frac{S_w}{S_c} = n\sqrt{\frac{1.42}{\pi}} \sqrt{\frac{k}{x_1}} \quad . \qquad \text{(V-4)}$$

The sum of S_w and S_c represents the total strength of the source. Therefore, the ratio of the amount of injected fluid still at the wall to the total of injected fluid is

$$\frac{S_w}{S} = \frac{1}{1 + \frac{1}{n}\sqrt{\frac{\pi}{1.42}}\sqrt{\frac{x_1}{k}}} \quad . \qquad \text{(V-5)}$$

Equation (V-5) is only an approximation since it is based upon the assumption that S_c is constant. Equation (V-5) shows there is on any level a continuous flux of injected fluid from the wall toward the core. Nevertheless, Eq. (V-5) not only indicated the general trend, but also gives reasonable values for $x_1 = 0$ ($S_w = S$) and $x_1 = \infty$ ($S_w = 0$) .

If it is assumed that the critical zone for overheating the refractory lining starts about 7' above the burner level and the cold

exhaust gas is injected 3' above the burner level, x_1 is 4' and S_w/S is approximately 0.26. That is, 74% of the injected fluid diffused into the porous medium. The remaining 26% is still in the wall region and available to protect the refractory in two ways: by replacing some of the oxygen-fuel mixture (i.e., reducing the heat release) and by cooling the gases developed in the combustion process.

Assuming that the temperature drop through the kiln wall is proportional to the heat release in the piping area, and that on the injection level 50% of the flow through the piping area is replaced by cold exhaust gases (i.e., on the 4' level considered, 13% of the flow in the piping area is cold exhaust gas) a reduction of the temperature drop through the kiln wall of approximately 13% could be achieved, resulting in a temperature drop on the wall inside of approximately 400 degrees Fahrenheit. This figure does not include the cooling effect, which might cause another drop, proportional to the ratio of cold injected gas to hot gases traveling along the wall and proportional to the temperature difference between the hot gases and the cold injected gases. This might, under the same assumption as above, result in a further temperature drop of approximately 300-400 degrees Fahrenheit.

Since the experiments of injection at the wall indicate that diffusion of the injected fluid into the porous media might be overestimated, i.e., that the injected fluid has a higher tendency to stay in the piping area along the wall, the estimation of a temperature drop along the refractory of about 700 degrees Fahrenheit might be conservative. This value was computed for an injection level 3' above the burner level and an injection rate of 50% of the gases traveling along the wall in the piping area.

CONCLUSIONS

The Friction Law

The pressure drop along the kiln can be computed according to Eq. (II-1)

$$\Delta p = f \frac{\rho V^2}{2} \quad \frac{L}{k}$$

where Δp = pressure drop

f = friction factor

ρ = density of gas

V = velocity in the core

k = controlling grain size

L = depth of the rock bed.

A reasonable f value for the presently used kiln feed material is 45. This value is strongly dependent upon the shape of the material.

The Diffusion Law

The diffusion process is described by Eq. (III-28)

$$\pi \frac{C}{S} V k x_1 = 1.42 \exp \left[- 1.42 \frac{r^2}{k x_1} \right]$$

where C = concentration

S = strength of the source

V = velocity in the core

k = grain size

x_1 = distance between injection point and observation plane in which concentration is determined

r = radial distance between injection axis and observation point at which concentration is determined.

Equation (III-28) proves the linearity principle, i.e., at a specific point the concentration is proportional to the strength of the source and inversely proportional to the velocity in the core.

Further, Eq. (III-28) proves the velocity independence of the diffusion process. The equation represents a Gaussian distribution with a standard deviation of

$$\sigma = 0.60 \sqrt{k x_1}$$

which will not change with velocity.

The principle of linear superposition was experimentally verified. This states that the diffusion process from one source is not influenced by simultaneous diffusion from other sources.

As far as the fuel concentration distribution in the kiln is concerned, the mirror effect at the kiln wall can be neglected for most practical purposes. For protection of the refractory from overheating, it seems to be useful to inject cold exhaust gas along the wall to reduce the amount of fuel-oxygen mixture in the wall zone and to produce a cooling effect.

FIGURES

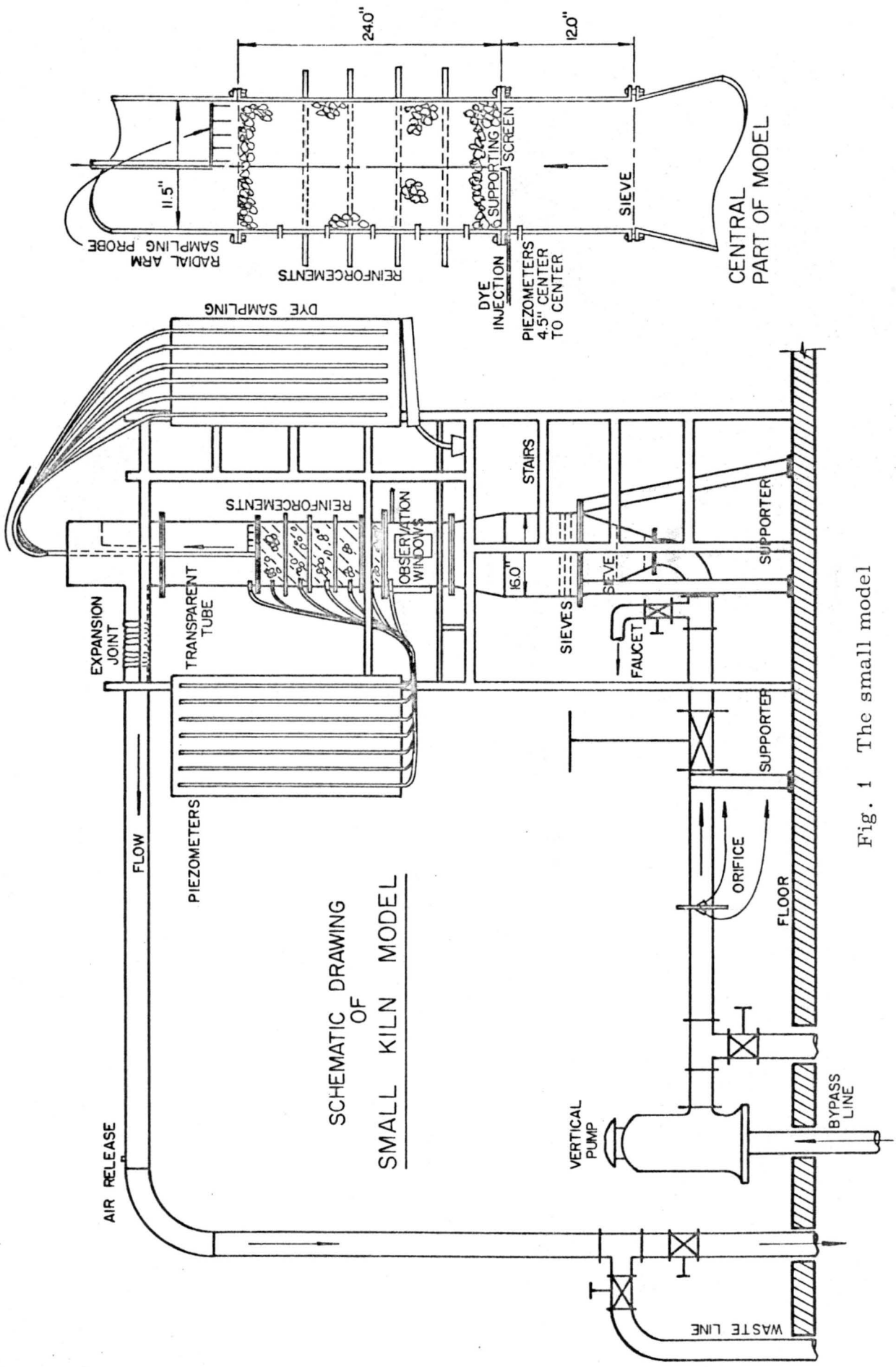

Fig. 1 The small model

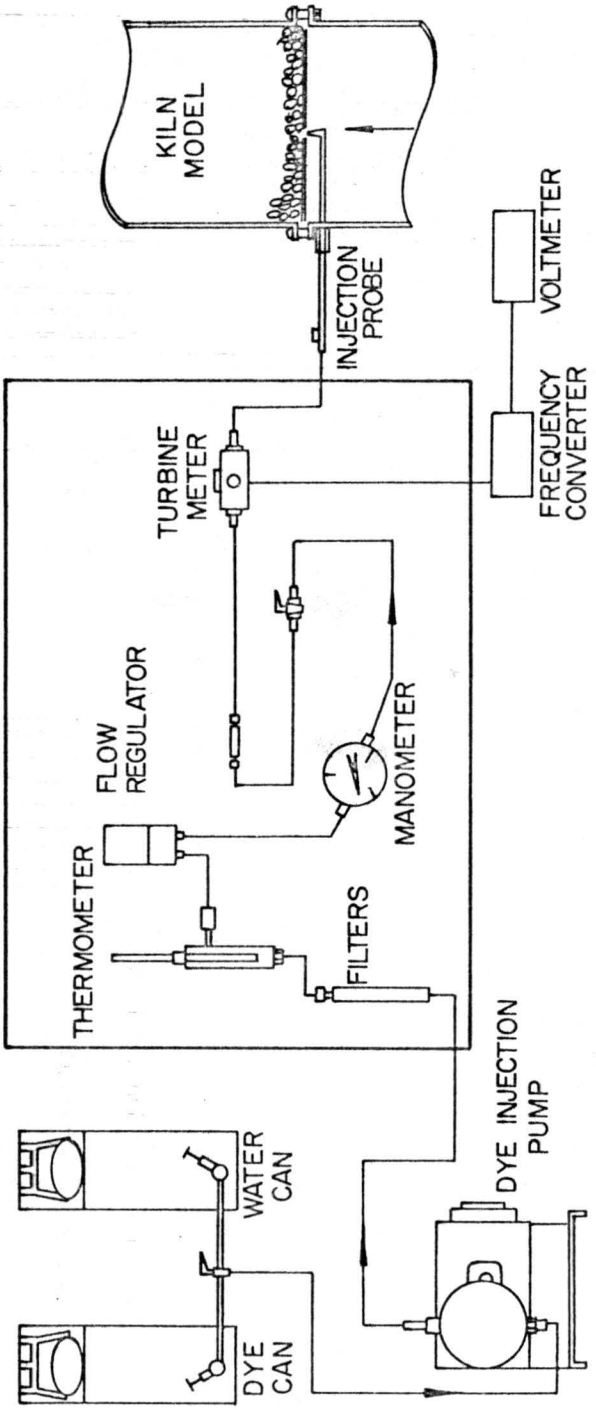

Fig. 2 Injection apparatus

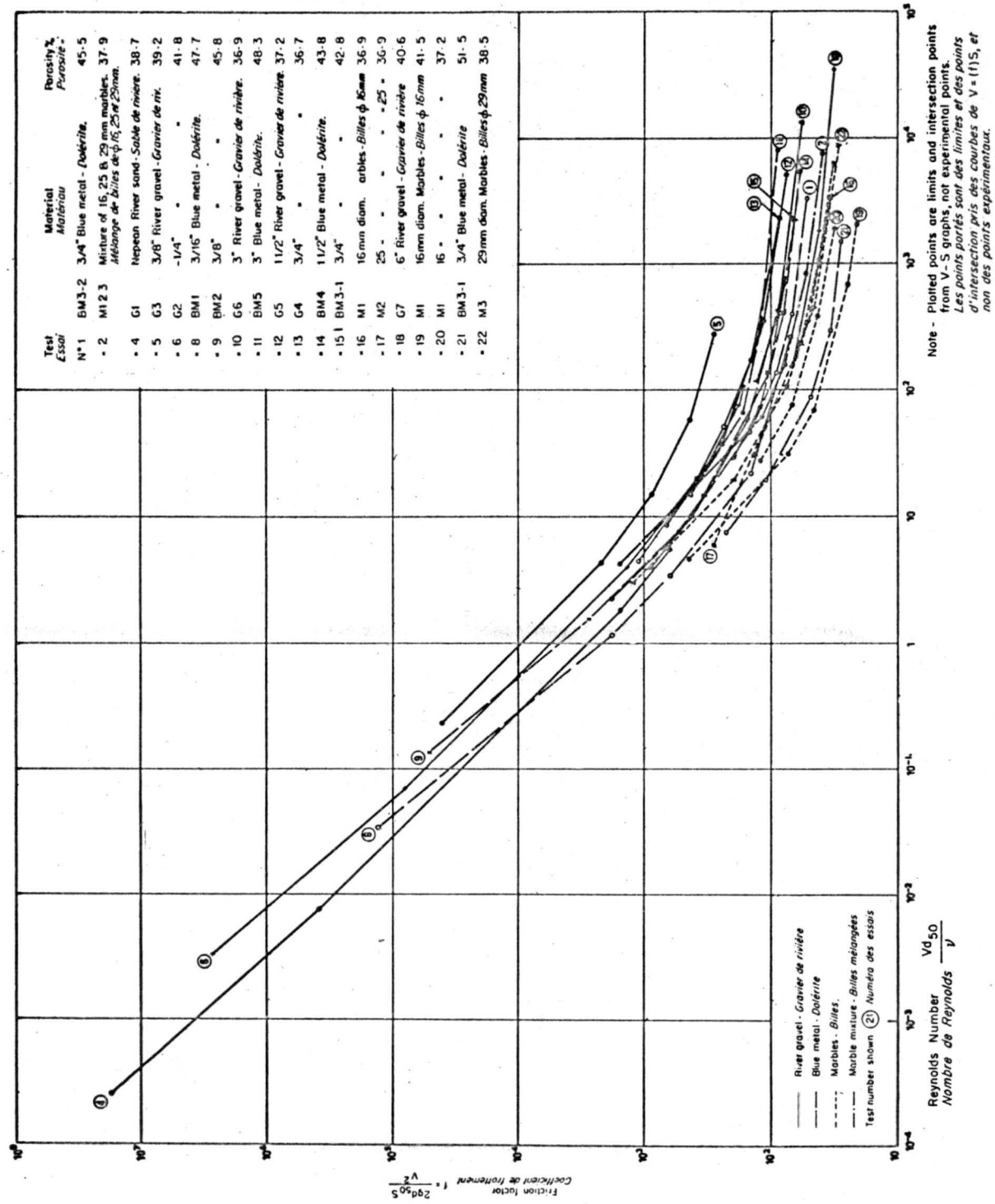

Fig. 3 Friction factor vs. Reynolds number
(according to Dudgeon)

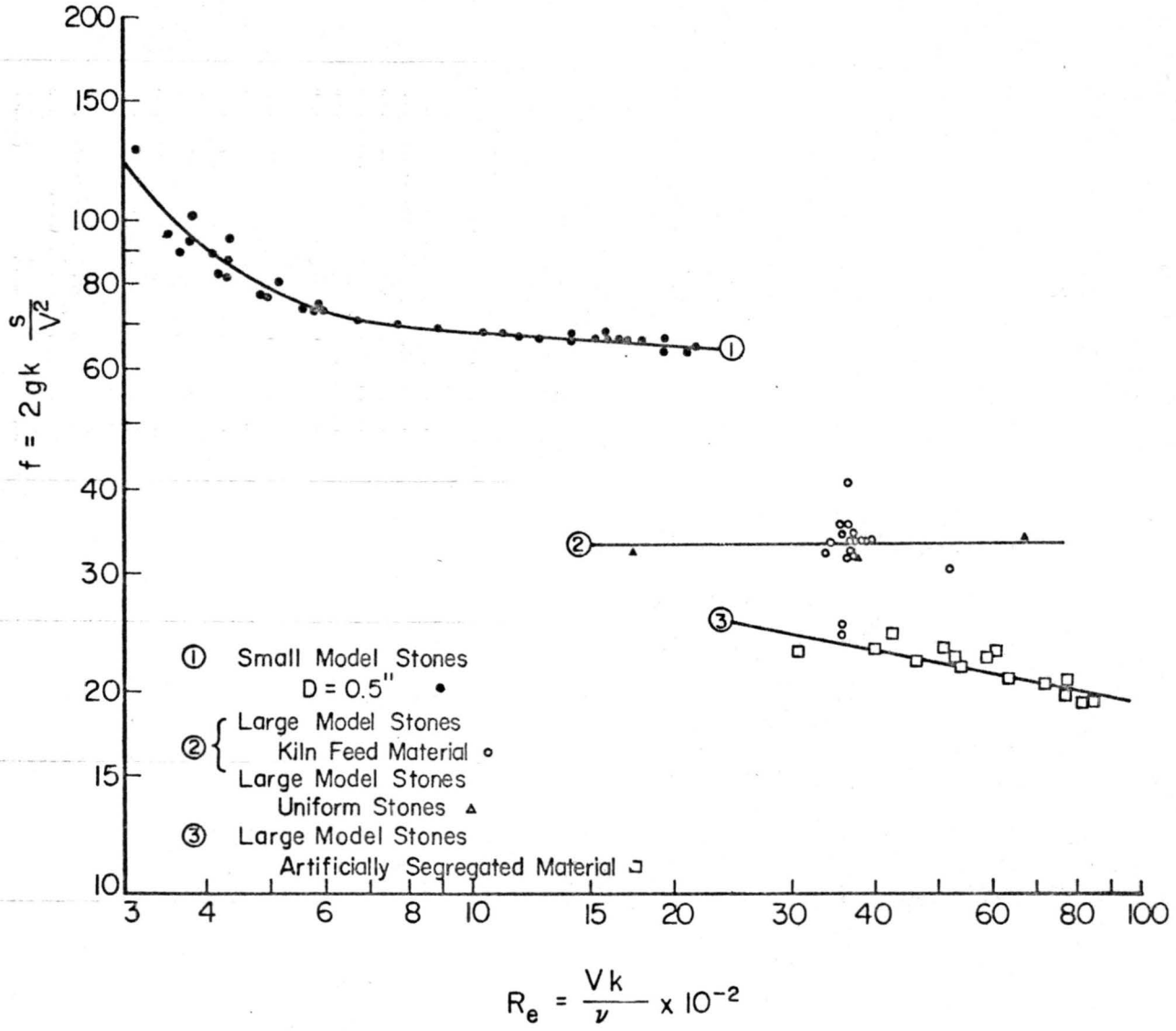

Fig. 4 Friction factor vs. Reynolds number for the experiments conducted at Colorado State University Engineering Research Center

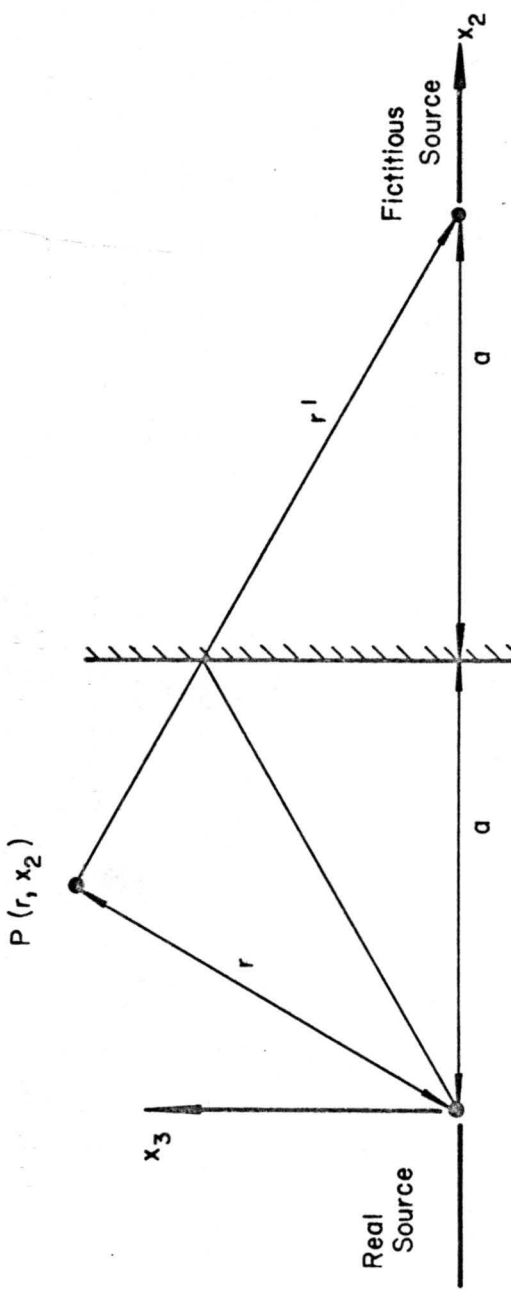

Fig. 5 Diffusion in the vicinity of a wall: definition sketch

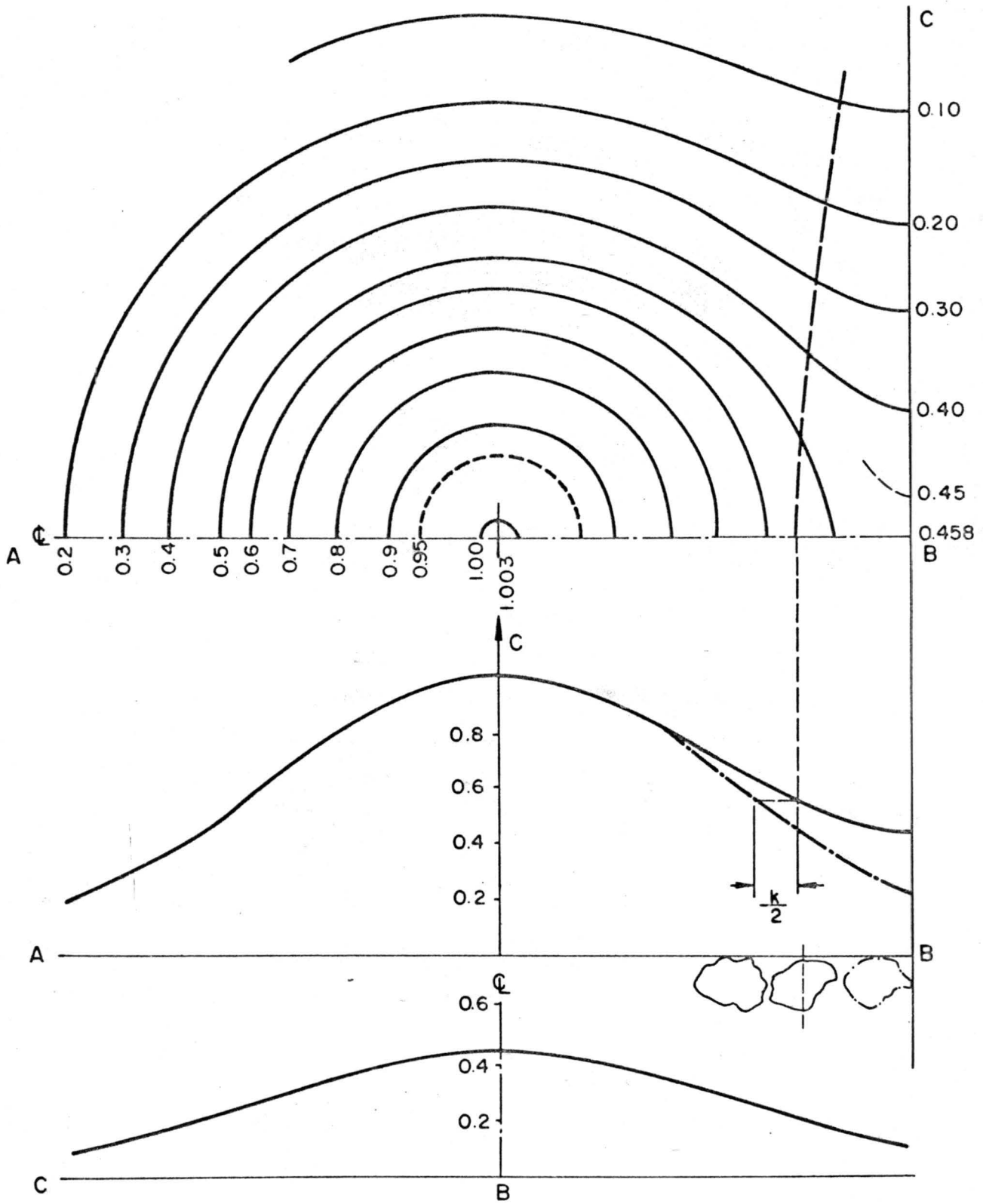

Fig. 6 Diffusion in the vicinity of a wall: lines of equal concentration on an 8 foot level with the injection point 1.5 feet from the wall (for presently used kiln feed material, neglecting the piping effect at the wall)

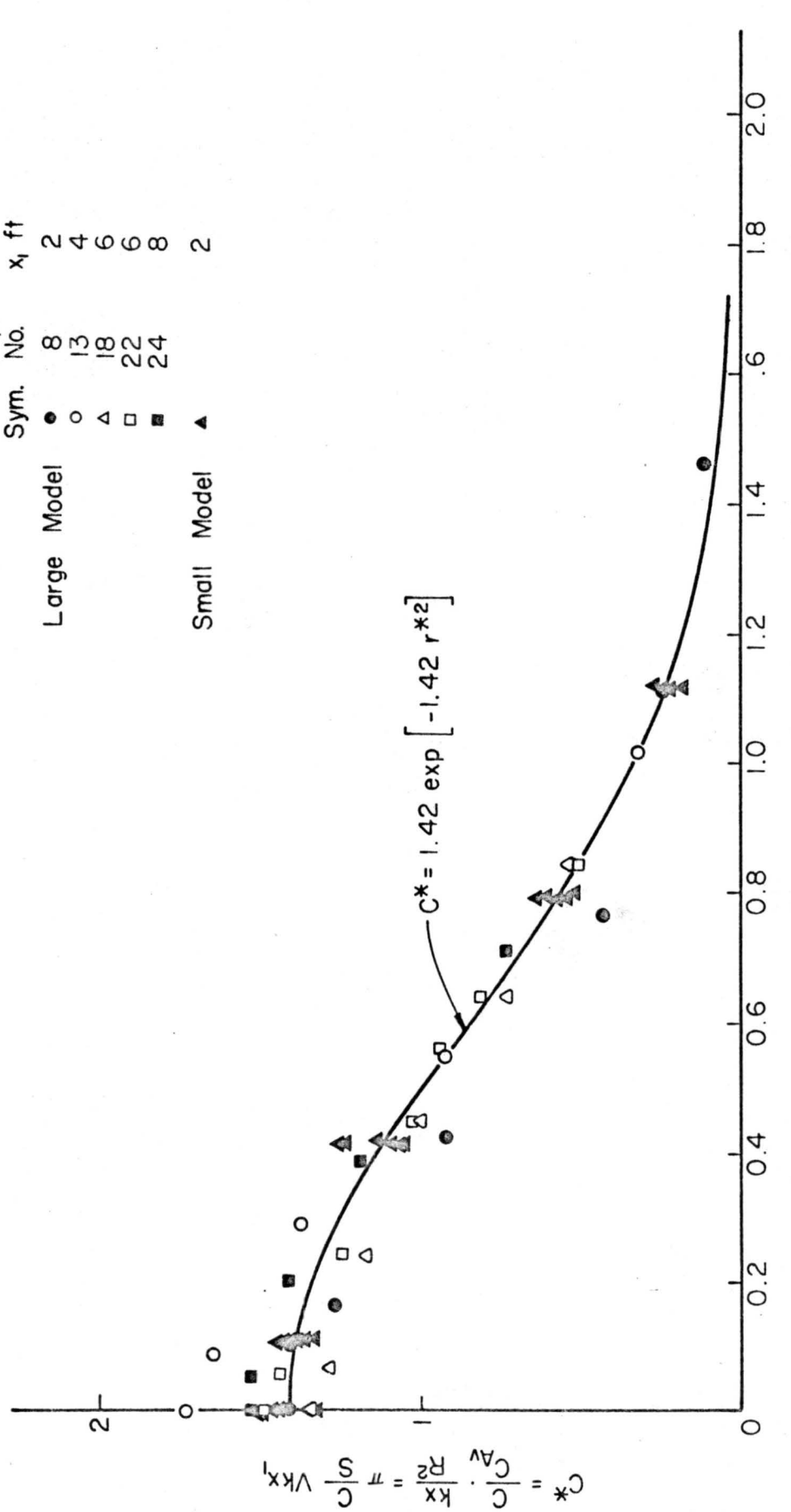

Fig. 7 Dimensionless concentration profile: observed points
The line represents Eq. (III-28)

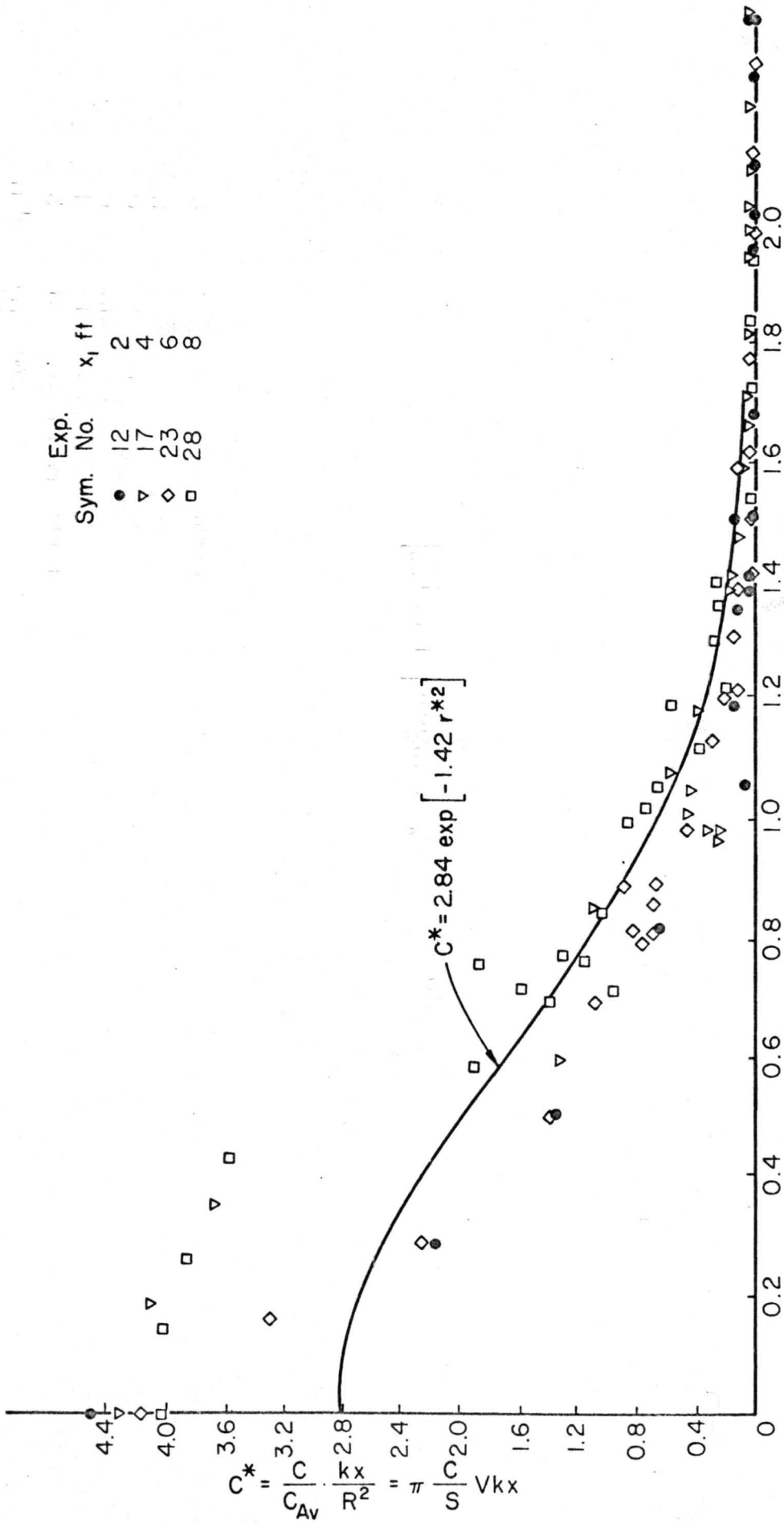

Fig. 8 Diffusion from a wall source

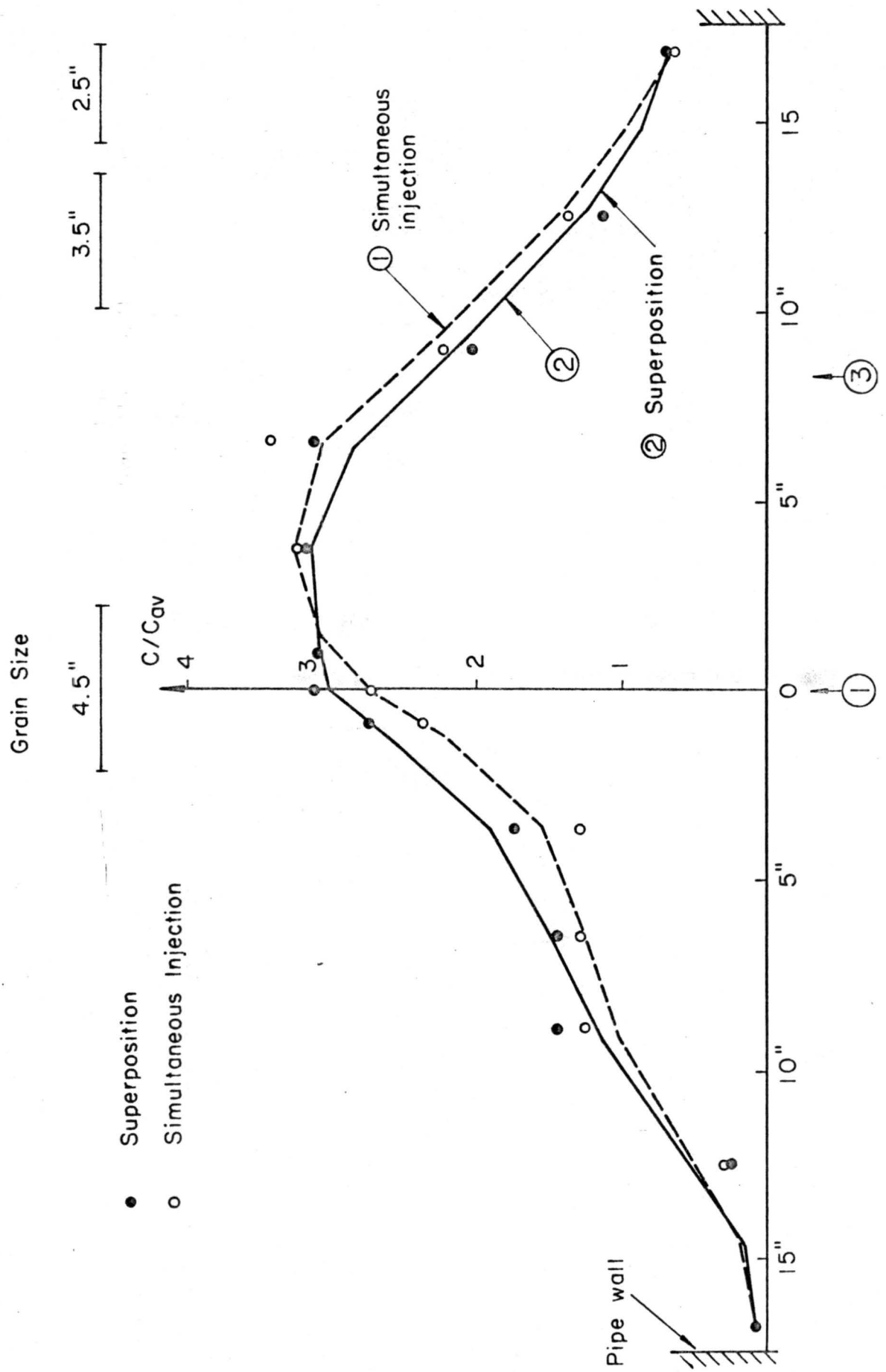

Fig. 9 Experimental verification of the law of linear superposition